

# A Robust Process for the Fabrication of Field Emission Backlights.

B. Marquardt, C. S. Cojucaru, S. Xavier\*, P. Legagneux\* and D. Pribat

LPICM, Ecole Polytechnique, CNRS, route de Saclay 91128 Palaiseau Cedex, France

\*Thales Research and Technology France, D128 91767 Palaiseau Cedex, France

## ABSTRACT

*In this paper, we present a novel process for the realization of large area, low cost field emission cathodes. The process makes use of alumina substrates, which are anodically oxidized in order to yield porous structures capable of hosting metal catalyst nanoparticles. By carefully controlling the final stage of the anodisation as well as the electrodeposition conditions, it is possible to fine tune the density of such catalysts in the range of  $10^8$ - $10^9$ /cm<sup>2</sup>. The catalytic growth of CNTs is subsequently performed at low temperature ( $\sim 600^\circ\text{C}$  or below, thanks to the use of  $\text{H}_2\text{O}$ ), using plasma enhanced chemical vapour deposition. There is no lithography need to make the cathode and current densities of  $\sim 1\text{mA}/\text{cm}^2$  are easily obtained.*

## 1. INTRODUCTION

Field emission from metal tips has been known and used for more than a century. Over the last three decades, field emission from micron-size metal tips has been intensively studied, particularly for the fabrication of field emission displays with low power consumption. In field emission displays (FEDs), arrays of microtips are fabricated using the well known Spindt technique [1]. More recently, multiwall carbon nanotubes (MWNTs) have emerged as a material of choice for field emission, also applicable to displays [2]. Because of their whisker-like shape, carbon nanotubes can exhibit field enhancement factors,  $\beta$ s, of around 250, larger than those of Spindt-type tips. Individual MWNT specimens can also emit larger currents (more than  $100\mu\text{A}$  without appreciable degradations [3]), although this is not really an issue as far as FEDs are concerned.

However, despite huge development efforts, FEDs have not yet made their way to the market place, probably because of fierce competition from PDPs and more recently from large AMLCDs.

Perhaps a more realistic and intermediate application for field emission over large areas would be backlights for AMLCDs. Field emission backlights are amenable to simple and inexpensive fabrication processes which are needed for such an application. This is probably an advantage over LED-based backlights which exhibit a

more complex structure.

Given the backlight application which we have in mind, we want to avoid the use of sophisticated and expensive MWNT synthesis processes involving, for instance, electron beam lithography for the definition of the catalyst particles [4, 5].

Here, we present a rather simple technique, that can be used to fabricate large area backlights using aluminum foils as substrates and avoiding any complex lithographic step. The technique also takes advantage of a low temperature plasma-enhanced chemical vapour deposition process that we are currently developing for the growth of vertically-aligned carbon nanotubes (see below).

## 2. LOW TEMPERATURE GROWTH OF MULTIWALL CARBON NANOTUBES

The preferred method for synthesising vertically aligned carbon nanotubes (CNTs) is dc plasma-enhanced chemical vapor deposition (dc-PECVD), using transition metal catalyst films/particles to seed and sustain the growth [5, 6].

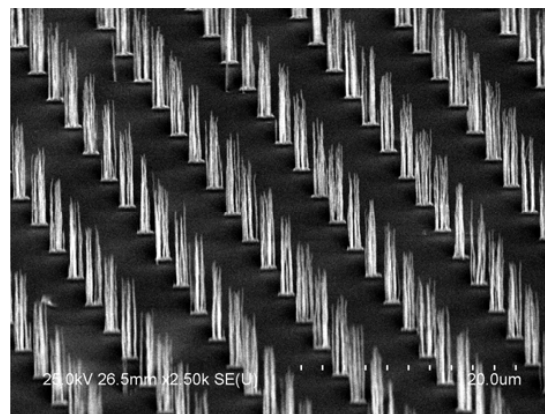


**Figure 1:** MWNTs grown by dc-PECVD at  $600^\circ\text{C}$ , using  $\text{H}_2\text{O}$  as a light oxidant (see text for details).

The plasma can be operated in the diode mode [6] or in the triode mode [7], the latter bringing more flexibility to the process. The growth temperature typically ranges

between 600 and 750°C depending on plasma chemistry.

Although CNT growth is a catalytic process and in principle gas phase decomposition only occurs on metal particles, there is always some kind of parasitic amorphous carbon deposition away from the catalysts. Also, the high flux of carbon-bearing species (radicals, ions ...) may lead to an early encapsulation and poisoning of the catalysts, thus halting the growth process. Therefore, some kind of etching species is needed in the plasma, in order to suppress or mitigate the parasitic deposition of amorphous carbon (a-C).

In the "classical" PECVD process,  $\text{NH}_3$  is added to the carbon bearing specie (usually  $\text{CH}_4$  or  $\text{C}_2\text{H}_2$ ), since it easily decomposes in the plasma, releasing atomic hydrogen (H). Atomic hydrogen, which is a well known scavenger for amorphous carbon, helps preventing the catalyst particles from being poisoned. However, the selective etching effect of H<sup>•</sup> seems to saturate after a certain CNT height (or growth time), depending on temperature, working pressure, gas flow...

Hence, it is rather difficult to obtain long CNT specimens. Also, the growth temperature with the  $\text{NH}_3$ -based mixture has to be around 700°C, in order to guaranty an acceptable crystalline quality for the CNTs.

We have developed a water-based growth process, where  $\text{H}_2\text{O}$  is employed (instead of  $\text{NH}_3$ ) for the purpose of etching a-C. This new process yields very long tubes and the growth rate shows no sign of saturation, even after long plasma exposure times. Figure 1 shows an example of localised growth, obtained from Ni pads ( $\sim 2\mu\text{m}$  in diameter), using a classical optical lithography aligner. For this particular experiment, we have used a mixture of  $\text{C}_2\text{H}_2$  and  $\text{H}_2\text{O}$  at a temperature of 600°C. CNTs over  $10\mu\text{m}$  long can be seen on this picture, corresponding to a 90 min growth time.

Another advantage of the  $\text{H}_2\text{O}$ -based process is that the growth temperature can be lowered, without inducing a significant degradation of the CNT's crystalline quality. Figure 2 shows some transmission electron microscope (TEM) views of MWNTs grown according to different chemistries. First of all, we point out that whether we use  $\text{NH}_3$  or  $\text{H}_2\text{O}$ , we still observe a tip-growth mechanism, where the catalyst particle stands at the tip of the CNTs. Second, the crystalline quality of the tubes is similar if not better for those specimens synthesized at 600°C, using  $\text{H}_2\text{O}$ .

Of course, the decrease of the growth temperature is of major importance, in order to use aluminum substrates as will be explained below. The introduction of water vapor in the plasma gas mixture seems to modify the growth mechanism<sup>[8]</sup>, since well crystallised MWNTs can be grown down to 550°C and even below<sup>[8]</sup>.

As explained above, the first role of  $\text{H}_2\text{O}$  is to replace  $\text{NH}_3$  for scavenging a-C. However, the role of water vapor is more complex and subtle, since oxygen released by  $\text{H}_2\text{O}$  decomposition in the plasma can probably saturate the catalyst particles, thus blocking carbon penetration and favouring surface diffusion which takes place (at appreciable rates) at much lower temperatures

than its bulk counterpart<sup>[8]</sup>. Figure 2-b also shows that the morphology of the  $\text{H}_2\text{O}$ -grown MWNTs is quite different from that of the  $\text{NH}_3$ -grown specimens. In particular, there are many more graphene layers in the  $\text{H}_2\text{O}$ -grown MWNTs and the facets of the Ni particles at the tip of MWNTs are much more pronounced and more regular suggesting a surface mechanism. As quoted above, the crystalline quality also seems better for the  $\text{H}_2\text{O}$ -grown MWNTs, although growth took place at a lower temperature, probably because no N atoms are incorporated in the MWNTs<sup>[9]</sup>. Finally, we note the presence of a thick amorphous layer on top of the Ni particle, which we identified as Ni oxide (fig. 2-c).

Although the interest of using small amounts of water vapor (in the few hundred ppm range) has already been shown for the thermal CVD growth of CNTs<sup>[10]</sup>, we emphasise here that the conditions for PECVD growth of CNTs using a mixture of hydrocarbons and  $\text{H}_2\text{O}$  are difficult to find, as discussed by Zhang *et al.*<sup>[11]</sup>.

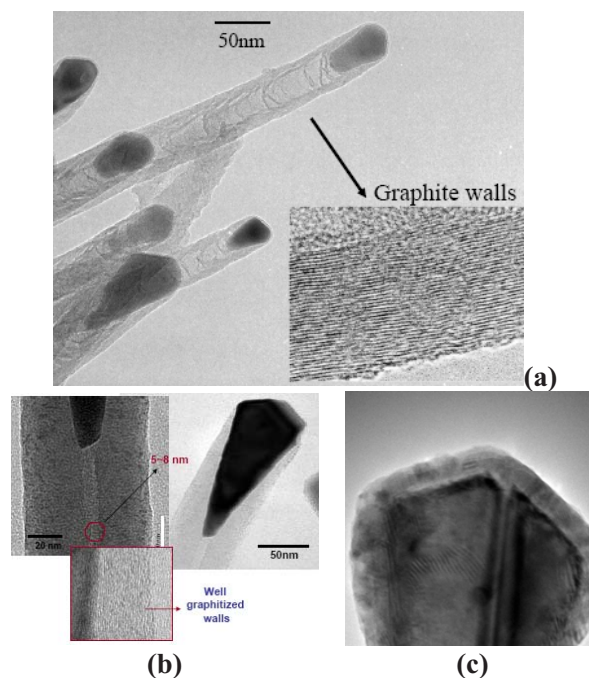
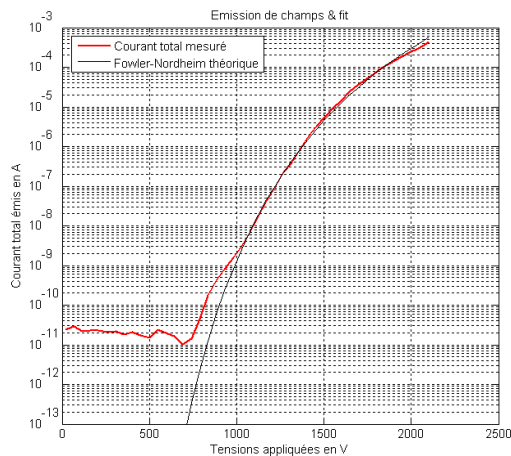


**Figure 2: TEM comparison between the nanostructure of MWNTs. (a): growth at 700°C using a mixture of  $\text{C}_2\text{H}_2 + \text{NH}_3$ . (b): growth at 600°C using a mixture of  $\text{C}_2\text{H}_2 + \text{H}_2 + \text{H}_2\text{O}$ . The MWNTs grown at 600°C with  $\text{H}_2\text{O}$  show a better crystalline quality, with more graphene walls. (c): a close view of the Ni particle at the top, showing a thick amorphous layer which we identify as nickel oxide.**

Fig. 3 presents field emission measurements performed on the  $\text{H}_2\text{O}$ -grown MWNTs. Arrays obtained by optical lithography ( $\sim 2\mu\text{m}$  diameter Ni dots) such as that shown in figure 1 were used for these field emission measurements. The emitted current density is typically around  $0.18\text{A}/\text{cm}^2$ , under an applied field of  $30\text{V}/\mu\text{m}$ . The oxidation layer at the tip, due to the  $\text{H}_2\text{O}$  effect at the growth temperature can explain this relatively low

value (see *e.g.*, ref. 3 for comparison). Although this current density is higher than what is needed for a backlight application, some specific approach to remove this layer is under test in our laboratory.

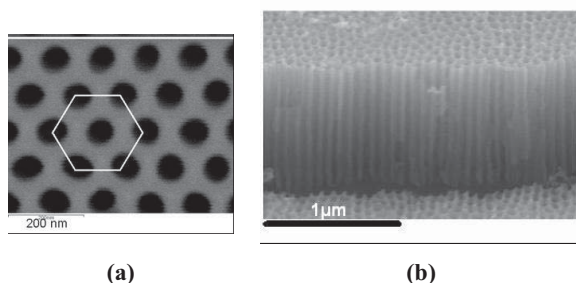
This being said, our interest here is to simplify as much as possible the cathode fabrication process. For this, we rely on the use of porous anodic alumina, a material that has been studied for almost 6 decades<sup>[12]</sup>.



**Figure 3:** MWNT field emission characteristic from an array of 7 mm<sup>2</sup>, (3mm diameter). The red curve is the actual measure of the field emitted current and the black curve is a Fowler-Nordheim fit.

### 3. POROUS ALUMINA TEMPLATES AND STRUCTURATION OF THE CATALYSTS

Porous anodic alumina (PAA) consists of an array of uniformly sized parallel pores. The electric field distribution at the pore tip (during anodic oxidation) explains pore nucleation. The porous structure is the result of an equilibrium process between field-assisted oxide dissolution at the oxide/electrolyte interface and oxide generation at the metal/oxide interface<sup>[13]</sup>. A two step anodic oxidation process has recently been shown to yield highly ordered honeycomb-like hexagonal arrays with a circular pore at the centre of each hexagon<sup>[14]</sup>.



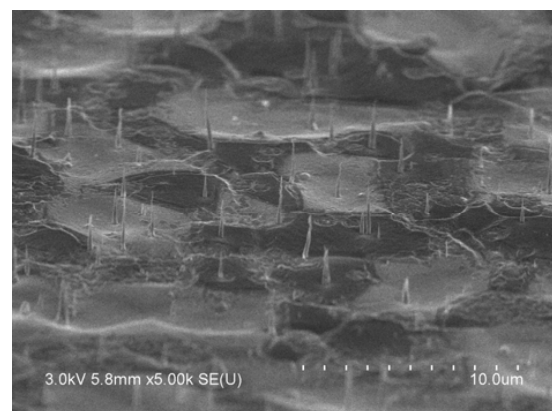
**Figure 4:** SEM viewgraphs of porous anodic alumina samples. (a) Top view; note the quasi perfect hexagonal self-organisation of the pores. (b) Cleaved view, showing how straight the pores are.

Figure 4 shows various pictures of PAA structures synthesised in our laboratory. The pore diameter and

interpore distance can be varied between a few nm and several hundred nm depending on the anodisation conditions (acid bath, voltage, temperature...). Such structures can be used as templates for the electrodeposition of metal catalysts (*e.g.*, Ni), where the catalyst diameter is shaped and determined by the pore's one. A major problem encountered with electrodeposition in PAAs is the penetration of the barrier layer at the bottom of the pores. In other words, it is very difficult to obtain uniform particle densities (or rather to control the particle density at all) unless particular tricks are employed.

We have recently developed a method for the precise control of the electrodeposition density inside the pores of PAA templates<sup>[15]</sup>. This method is based on the combination of anodization control, particularly in its final stage, and low voltage electrodeposition. Briefly, the idea is to use an exponential voltage decrease (as a function of time) at the end of the anodisation step. By carefully choosing the time constant of the exponential voltage decrease, it is possible to slightly amplify the natural thickness variations of the barrier layer. Now, if electrodeposition is performed at low voltage, metal particles will only be deposited in those pores with a small barrier thickness, at the expense of the others (see ref. 15 for details). This opens up the possibility of tuning and controlling the metal particle density in PAA. After electrodeposition of the particles, the PAA membrane can be selectively dissolved, leaving nanometer-sized metal particles of predefined density, randomly distributed on the surface of the underlying aluminum foil.

Once the catalyst particles obtained, the growth of vertically-aligned CNTs can be performed, using the low temperature (*i.e.*, compatible with an Al substrate) H<sub>2</sub>O-based PECVD method. The advantage is that there is no need for fine (and expensive) lithography steps for catalyst definition. The overall process is compatible with large areas, as long as PECVD reactors already exist for the production of AMLCD backplanes and aluminum substrates can be found in large foils.



**Figure 5:** Vertically aligned MWNTs grown on an aluminum foil by dc-PECVD at 575 °C in the presence of H<sub>2</sub>O.

Figure 5 shows a picture of vertically-aligned CNTs after PECVD growth (at 575°C, using the H<sub>2</sub>O-based process described above) from Ni particles that had been deposited to a density of  $\sim 10^9/\text{cm}^2$ . The random organization of the Ni particles leads to a random distribution of the CNTs, with an average spacing between 3 and 5  $\mu\text{m}$ . We observe a  $\sim 10^3$  ratio between the Ni particle density before growth and the actual CNT density after growth (a few  $10^6/\text{cm}^2$ ), probably because some of the Ni catalysts are poisoned by the underlying aluminium, alloying with it during the 575°C temperature bake. Also, during growth, the Al surface seems to get damaged, which increases the surface roughness. Although this surface roughness is probably not detrimental, a proper *in-situ* annealing treatment is under development in order to minimise it.

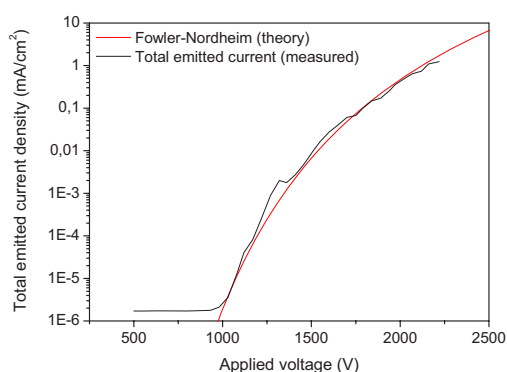


**Figure 6: Field emission characteristics of a 7 mm<sup>2</sup> random MWNT array. The black curve shows the actual measurement and the red curve is a Fowler-Nordheim fit.**

Figure 6 shows the field emission characteristics of the random MWNT array shown in figure 5. Typical current values are of the order of  $1\text{mA}/\text{cm}^2$  at  $\sim 30\text{V}/\mu\text{m}$  applied field, comparable to values obtained with random arrays of metal nanowires with a density of  $10^7/\text{cm}^2$  [16]. However these emitted current values are much smaller than those measured on MWNT arrays grown in the same way, but organised by lithography (see fig. 3 above). The random organization of the CNTs is probably not as efficient as the lithography-based one for minimizing lateral screening effects [17]. We believe that we will be able in the near future to improve the current density by (i) increasing the density of Ni nanoparticles, changing the time constant of the exponential voltage decrease at the end of the anodization step (see ref. 15) and (ii) decreasing the amount of Ni nanoparticles poisoned by the substrate by a proper treatment before growth.

#### 4. CONCLUSION

We have presented a novel approach for the low cost fabrication of field emitter arrays using multiwall carbon nanotubes grown by plasma-enhanced chemical vapor

deposition in a C<sub>2</sub>H<sub>2</sub>/H<sub>2</sub>O atmosphere. The Ni catalyst nanoparticles have been deposited prior to CNT growth inside porous alumina templates synthesized by anodic oxidation. These templates were prepared by carefully decreasing the anodization voltage according to an exponential law, yielding a perfect control on the density of electrodeposited Ni nanoparticles. The overall process is very simple, with no critical lithographic step and it is totally compatible with large areas. The field emitted current density is typically in the  $\text{mA}/\text{cm}^2$  range for applied electric fields of  $30\text{V}/\mu\text{m}$ , which should be appropriate for backlighting applications. We presently work on increasing the emitted current density.

#### 6. REFERENCES

- [1] See *e.g.*, C. Spindt, I. Brodie, C.E. Holland and P.R. Schwoebel, in « Vacuum Microelectronics », W. Zhu Ed., Wiley, 2001.
- [2] D. S. Chung, S. H. Park, H. W. Lee, J. H. Choi, S. N. Cha, J. W. Kim, J. E. Jang, K. W. Min, S. H. Cho, M. J. Yoon, J. S. Lee, C. K. Lee, J. H. Yoo, Jong-Min Kim, J. E. Jung, *Appl. Phys. Lett.*, **80**, 4045 (2002).
- [3] E. Minoux *et al.*, *Nano Lett.*, **5**, 2135 (2005).
- [4] see *e.g.*, V. I. Merkulov, D. H. Lowndes, Y. Y. Wei, G. Eres, and E. Voelkl, *Appl. Phys. Lett.*, **76**, 3555 (2000)
- [5] K. Teo, R. Lacerda, M.H. Yang, A.S. Teh, L. Robinson, S.H. Dalal, N. Rupesinghe, M. Chhowalla, S.B. Lee, D. Jefferson, D. Hasko, G. Amaratunga, W. Milne, P. Legagneux, L. Gangloff, E. Minoux, J.P. Schnell and D. Pribat, *IEE Proc.-Circuits Devices Syst.*, **151**, 443 (2004).
- [6] A.V. Melechko, V.I. Merkulov, T.E. McKnight, M.A. Guillorn, K.L. Klein, D.H. Lowndes and M.L. Simpson, *J. Appl. Phys.*, **97**, 041301 (2005).
- [7] S. H. Lim, K. C. Park, J. H. Moon, H. S. Yoon, D. Pribat, Y. Bonnassieux and J. Jang, *Thin Solid Films*, **515**, 1380 (2006).
- [8] C.S. Cojocaru *et al.*, to be published.
- [9] M. Glerup, M. Castignolles, M. Holzinger, G. Hug, A. Loiseau, P. Bernier, *Chemical Communications* **20**: 2542-2543 (2003).
- [10] K. Hata, D.N. Futaba, K. Mizuno, T. Namai, M. Yumura, and S. Iijima, *Science*, **306**, 1362 (2004).
- [11] G. Zhang, D. Mann, L. Zhang, A. Javey, Y. Li, E. Yenilmez, Q. Wang, J.P. McVittie, Y. Nishi, J. Gibbons and H. Dai, *Proc. Nat. Acad. Sci.*, **102**, 16141 (2005).
- [12] F. Keller, M.S. Hunter, D.L. Robinson, *J. Electrochem. Soc.*, **100**, 411 (1953).
- [13] J.P. O'Sullivan and G.C. Wood, *Proc. Roy. Soc. Lond.*, **A 317**, 511 (1970).
- [14] H. Masuda and K. Fukuda, *Science*, **268**, 1466 (1995).
- [15] B. Marquardt *et al.*, *Nanotechnology*, **19**, 405607 (2008).
- [16] S. Xavier *et al.*, *Nanotechnology*, **19**, 215601 (2008).
- [17] L. Nilsson, O. Groening, C. Emmenegger, O. Kuettel, E. Schaller and L. Schlapbach, *Appl. Phys. Lett.*, **76**, 2071 (2000).